



**UNIVERSITY
OF TURKU**

Analysis of teaching laboratory using commercial motor design software

Department of Mechanical and Materials Engineering

Bachelors's thesis

Author:

Miro Vesterinen

14.5.2025

Turku

The originality of this thesis has been checked in accordance with the University of Turku quality assurance system using the Turnitin Originality Check service.

Bachelor's thesis

Subject: Mechanical Engineering

Author: Miro Vesterinen

Title: Analysis of teaching laboratory using commercial motor design software

Supervisor: Prof D G Dorrell

Number of pages: 30 pages

Date: 14.5.2025

The purpose of this thesis is to analyse teaching laboratory using commercial motor design software. During this thesis, the most common electrical motor in the industrial world, a three-phase induction motor, is analysed. This thesis focuses on a motor with a squirrel cage rotor. The first literature review presents the motor, tests for determining parameters for the motor model and the working principle of the motor.

De Lorenzo's semi-automatic electric machines laboratory is used for experimental work. No-load, locked-rotor, load, and direct current resistance tests are conducted on the motor and measurements are taken. After that, the MATLAB program is coded to calculate the desired parameters. After that, the same motor is modelled with Simcenter SPEED by Siemens. Also, plots are created with data from MATLAB and SPEED. Parameter values between modelling and experimental are compared and analysed.

Key words: Simcenter SPEED, MATLAB, induction motor, modelling, electric machines laboratory, De Lorenzo, squirrel cage rotor

List of used symbols:

s	slip	%
N	actual speed of the rotor	rpm
N_s	synchronous speed	rpm
R_1	stator winding resistance	Ω
R_2	rotor resistance	Ω
R_c	core loss resistance	Ω
R_{LR}	locked-rotor resistance	Ω
V_{DC}	stator direct current voltage	V
V_1	stator phase voltage	V
V_{th}	Thévenin's voltage	V
I_{DC}	stator direct current	A

I_1	stator current	A
I_0	exciting current	A
I_2	rotor current referred to the stator	A
P_{rot}	rotational losses	W
P_{NL}	three-phase no-load power	W
P_{core}	core losses	W
P_{in}	electrical input power	W
P_{out}	mechanical output power	W
P_{LR}	three-phase locked-rotor power	W
X_m	magnetizing reactance	Ω
X_{NL}	no-load reactance	Ω
X_{LR}	locked-rotor reactance	Ω
X_1	stator leakage reactance	Ω
X_2	rotor leakage reactance	Ω
E	electromotive force (EMF)	V
Z_{LR}	impedance of the equivalent circuit	Ω
Z_{th}	Thévenin's impedance	Ω
f_{LR}	lower frequency	Hz
f_n	rated frequency	Hz
S_{NL}	three-phase no-load apparent power	W
S_{LR}	three-phase locked-rotor apparent power	W
Q_{NL}	no-load reactive power	VAR
Q_{LR}	locked-rotor reactive power	VAR
T	torque	Nm
η	efficiency	%

Table of contents

1	Introduction	5
2	Literature review	6
2.1	Three-phase induction motor construction and components	6
2.1.1	Construction	6
2.1.2	Stator	6
2.1.3	Squirrel cage rotor	7
2.2	Working principle of three-phase induction motor	8
2.3	Direct Current Resistance Test	9
2.4	No-Load Test	10
2.5	Locked-Rotor Test	12
2.6	Load Test	13
2.7	Thévenin's theorem	14
3	Experimental Setup	15
3.1	Experimental equipment	15
3.2	Procedure	16
3.2.1	Test procedure	16
3.2.2	Modelling	16
3.2.3	Results analysis	17
4	Results	18
5	Discussion	21
6	Conclusion	22
7	References	23
	Appendices	25
	Appendix 1. Simcenter SPEED design sheets	25
	Appendix 2. The MATLAB code	26

1 Introduction

Three-phase induction motors are widely used and the most common electrical motor in the industrial world. Three-phase induction motor advantages are high reliability, simple and robust construction, easy and low maintenance, low cost and high overload capacity.[1–3] Due to these advantages, the motor remains highly popular despite the increasing popularity of other motor technologies in the industry [2]. Despite its many advantages, the three-phase induction motor has some drawbacks, such as low starting torque, low power factor and high inrush current [1].

Four tests are generally conducted to determine the parameters of a three-phase induction motor model: a no-load test, a locked-rotor test, a direct current resistance test, and a load test. [4,5] During this thesis, the operation and structure of the three-phase induction motor are examined. Those four tests are conducted, and motor model parameters are calculated with the MATLAB program. For testing, the De Lorenzo semi-automatic electric machines laboratory was used. After the experimental work, the same motor was modelled using Siemens Simcenter SPEED. The results are compared, and conclusions are drawn based on them.

While writing this thesis, the author used ChatGPT by OpenAI and Grammarly by Grammarly Inc. to check and improve the English language. While using the tools, the author checked and fixed the text and takes full responsibility for the thesis content.

2 Literature review

2.1 Three-phase induction motor construction and components

2.1.1 Construction

Essentially, the induction motor is made up of two primary components. The stator is a stationary part of the motor, and the rotor is a rotating part of the motor. With a narrow air gap, the rotor is isolated from the stator. There are two types of rotors: the squirrel cage rotor and the wound rotor.[6] This thesis focuses on the squirrel cage rotor.

2.1.2 Stator

The stator core and frame are two main parts of the stator. The stator frame is the external casing of the motor, and the core and winding are supported by the frame. There are multiple forms of the stator frame due to the operating conditions, and motor cooling is related to the frames. A few motor examples are totally enclosed nonventilated (TENV), where the motor is totally enclosed and cooling does not require an external fan, totally enclosed fan-cooled (TEFC) where the motor is totally enclosed but needs an external fan for cooling and open drip-proof (OPD) where the ventilation openings prevent the entry of substances and liquids coming towards the motor at a certain angle into the motor.[5]

The rotating magnetic field is produced by the stator core, which carries three-phase windings [5]. The main material of the winding is copper or aluminium [7]. The six terminals of the windings are connected by a junction box, with two terminals for each phase [5]. The stator is wound to stator slots for a specific number of poles based on the speed [5,6]. The Stator can be star or delta-connected, and when a three-phase power supply energises the stator winding, it generates a rotating magnetic field (RMF) [6]. The core is laminated with 0.3-0.6 mm-thick steel stampings that are isolated from each other. The stampings are designed with slots for windings and are attached to the stator frame. Stamping material is generally high-grade silicon steel because this material reduces hysteresis losses.[5] Hysteresis refers to the extent of magnetisation or flux density that trails behind the magnetising force due to molecular friction[8]. Core lamination is done to reduce eddy current losses[5]. Eddy currents are caused by a voltage induced in the iron core of electromagnets. Eddy currents resist the current, producing the magnetic field [8]. The structure of the stator is illustrated in Figure 1.

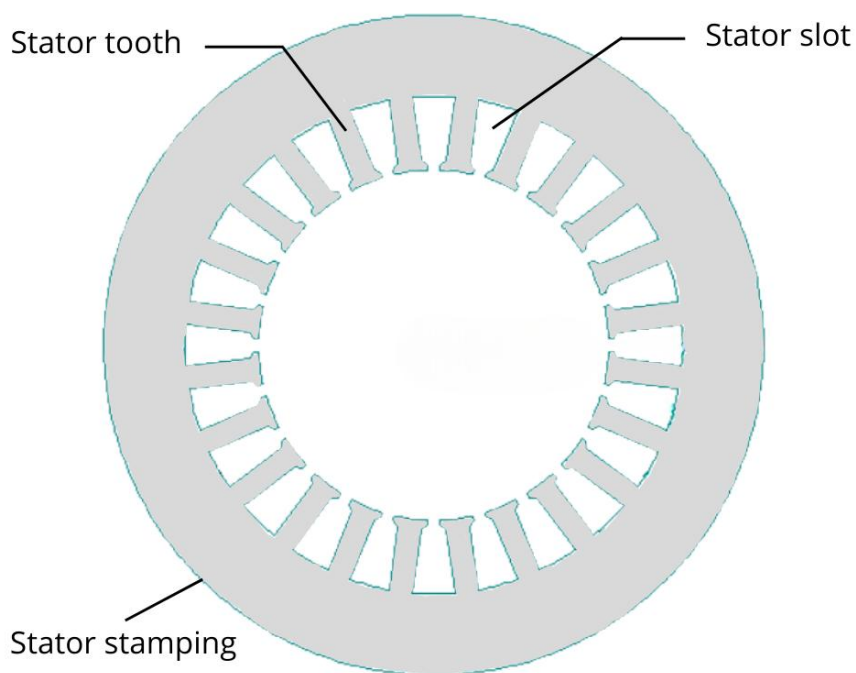


Figure 1. Structure of the stator of an induction motor.

2.1.3 Squirrel cage rotor

The structure of the squirrel cage rotor is relatively straightforward. Bars of the rotor are placed into the slots of the electrical steel laminated cylinder. There is no insulation layer between the rotor steel and bars because the voltage developed in the squirrel cage winding is very low. Bars are attached and permanently short-circuited with aluminium or copper conducting rings, which are also called end-rings.[5,9,10] Bars are electrically braced, welded or bolted to end-rings. The end-rings and the bars attached to them form a closed circuit, which resembles a squirrel cage.[5,10] Usually, the rotor bars are skewed relative to the axis of the shaft. By skewing the bars, magnetic hum can be reduced, keeping the motor quiet and magnetic locking, or cogging, between the rotor and stator can be prevented.[5,6] The resistance of the whole rotor is small, and there is no external resistance added [6]. The structure of the squirrel cage rotor is illustrated in Figure 2.

The squirrel cage rotor bars need to meet metallurgical, mechanical and thermal requirements. Aluminium is preferred when a strong starting capability is needed with a limited starting current. Much more expensive copper bars are used for low and medium starting torques. A rotor with copper bars can achieve better mechanical efficiency because copper has over 60% better conductivity than aluminium.[11]

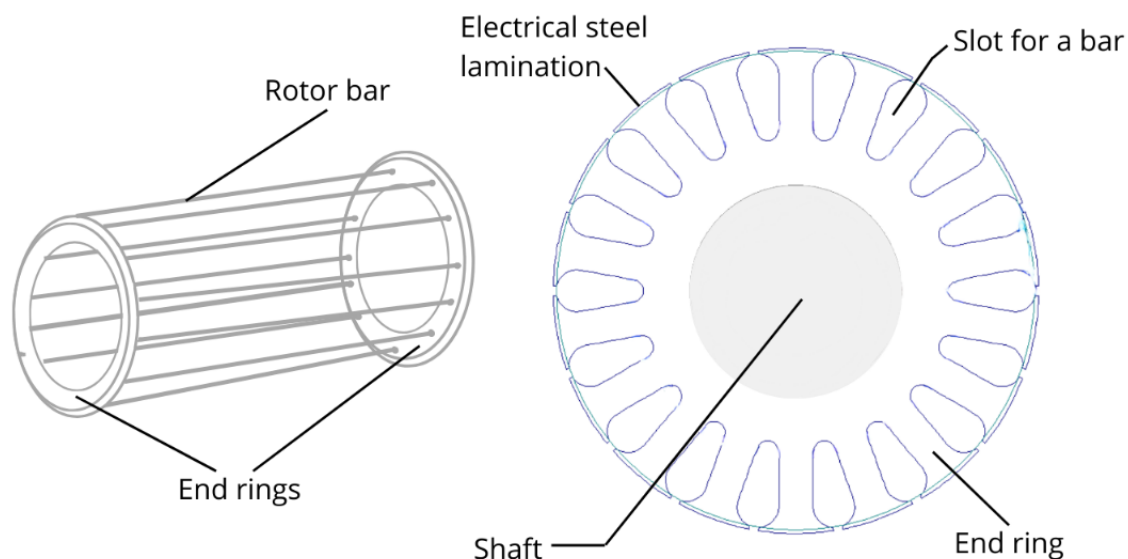


Figure 2. Structure of the squirrel cage rotor.

2.2 Working principle of the three-phase induction motor

The operation of a three-phase induction motor is based on Faraday's law of electromagnetic induction. Three-phase power supply is connected to an induction motor, and the current in the stator windings generates a rotating magnetic field (RMF) in the air gap, whose speed is the motor's synchronous speed. This speed depends on the frequency of the power supply and the number of poles the stator has. To provide optimal performance, the power source phase difference is usually 120 degrees.[4–6,12]

Rotor windings are cut by the RMF, and the electromotive force (EMF) is induced in the rotor windings. Induced EMF causes the currents to circulate in the short-circuited rotor. When the rotor rotates, the stator currents' synchronous frequency is higher than the rotor currents' frequency. [4,5] According to Ampere's law, circulating currents produce the magnetic field. There are now two magnetic fields, rotor field and stator field (RMF), which interact is crucial for motor operation. With a phase difference, both of them are rotating at synchronous speed. As a result, the two fields generate a constant torque that accelerates the rotor in the direction of the RMF of the stator.[4–6] Figure 3 illustrates the operating principle.

Rotor speed is always slightly less than synchronous speed. Because without relative speed between the RMF and the rotor, no EMF is induced in the rotor, resulting in no current flow

through the rotor, and consequently, the torque produced by the motor is zero.[4,6] Due to the rotor rotating at a lower speed than synchronous speed, an induction motor is also called an asynchronous motor. The difference between the synchronous speed and the rotor speed is called a slip. Slip is typically 2–5% with small motors and increases when the load of the induction motor increases.[6,13,14] The slip s is calculated as follows, where N_s is the synchronous speed and N is the actual speed of the rotor [6].

$$s = \frac{N_s - N}{N} \quad (1)$$

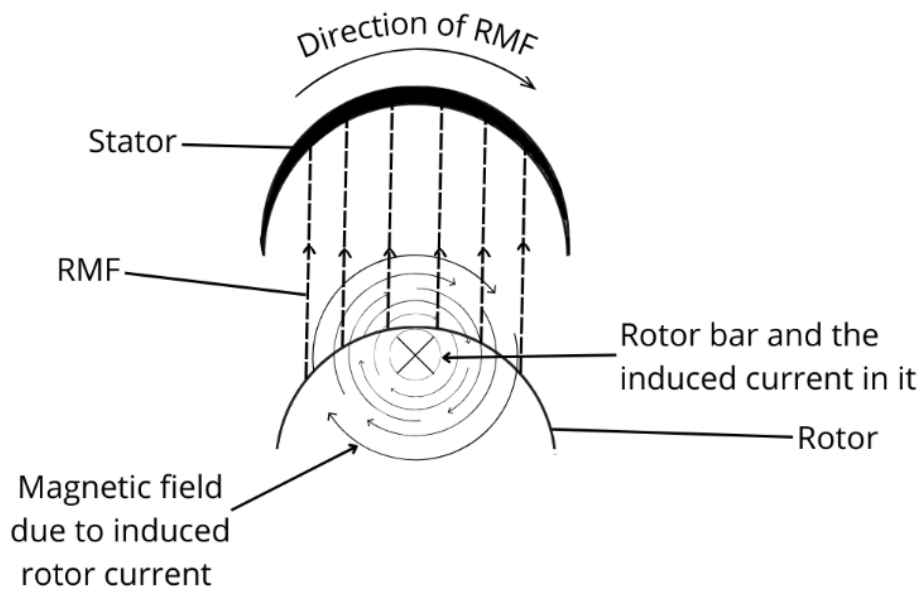


Figure 3. Working principle of an induction motor

2.3 Direct Current Resistance Test

The stator winding resistance R_1 can be found with a direct current (DC) resistance test. There is no induced rotor voltage or potential difference across the inductances, and the motor parameters will be limited to the resistance of the stator winding. The test is performed by applying a known DC voltage across two stator terminals and measuring the current. [5,15] The stator DC resistance can be calculated with Ohm's law, but the calculation depends on how the stator winding is connected. If the test is also performed for the other two terminal

sets, then the average of all terminal sets is used as R_1 . [15,16] Formulas for star and delta connections are shown below [15].

$$R_{1,star} = \frac{1}{2} \frac{V_{DC}}{I_{DC}} \quad (2)$$

$$R_{1,delta} = \frac{3}{2} \frac{V_{DC}}{I_{DC}} \quad (3)$$

2.4 No-Load Test

Core loss resistance R_c , friction and windage losses, which are called rotational losses P_{rot} and magnetising reactance X_m are obtained with the no-load test. During the no-load test the stator voltage V_1 , the stator current I_1 and the three-phase power P_{NL} are measured. [5] The test is performed by applying rated three-phase voltage and frequency to the stator winding, and the rotor is kept disconnected from any shaft of the driven equipment. [17]

Rotational losses P_{rot} can also be determined with another test. During the test, the rotor of the induction motor is driven by another machine. The machine speed is the same as the induction motor rotor's actual speed during a no-load test. Rotational losses are the difference between the machine's output power with and without an induction motor. [5]

During the no-load test, the motor runs close to a synchronous speed. In these conditions, slip is approaching zero, and the rotor resistance value is high. This causes the rotor current value to fall significantly smaller than the magnetising current, and as a result, the rotor copper losses can be neglected. [5,17] Induction motor magnetising path includes the airgap which exciting current I_0 is around 25–50% of its rated current, causing that the joule losses $3RI^2$ cannot be neglected in the stator. The magnetising branch is bypassed by a rotor branch with high impedance, resulting in a parallel impedance that closely approximates that of the magnetising branch. This condition causes the stator current I_1 to be nearly equal to the excitation current I_0 . [5]

Stator losses $3R_1I_1^2$, hysteresis and eddy current losses which are referred to as core losses $P_{core} = 3 \frac{E^2}{R_c}$ and rotational losses P_{rot} together constitute the total losses in the motor at no-load, which is the measured three-phase input active power P_{NL} . Stator per phase direct

current (DC) resistance value R_1 , should be corrected for the winding temperature during the test. The skin effect on the stator resistance value is minimal, even though the stator frequency always matches the line frequency. The skin effect accounts for approximately 5–15% of the Joule losses in the stator resistance. Usually, these are neglected, and the stator resistance is considered as its DC value.[5]

Let E denote the electromotive force (EMF) induced in the stator winding by the rotating flux under no-load conditions, which is approximately given by $E \approx V_1 - I_1 X_1$, representing the voltage across the parallel branch. Using value for X_1 from locked-rotor test, the E is obtained. Based on this, the equations for the input active power P_{NL} and reactive power Q_{NL} at no-load and the core loss at rated voltage P_{core} are as follows.[5]

$$P_{NL} = 3I_1^2 R_1 + 3 \frac{E^2}{R_c} + P_{rot} \quad (4)$$

$$Q_{NL} = 3I_1^2 X_1 + 3 \frac{E^2}{X_m} \quad (5)$$

$$P_{core} = P_{NL} - 3I_1^2 R_1 - P_{rot} = 3 \frac{E^2}{R_c} \quad (6)$$

From this, it can be derived that the R_c is calculated as follows [5].

$$R_c = 3 \frac{E^2}{P_{core}} \quad (7)$$

The removal of the core loss resistance R_c from the parallel branch, along with the corresponding subtraction of the core loss from the internal mechanical power P , leads to some simplification without introducing significant error. This approach effectively combines the core loss with the rotational losses. This method has the advantage of eliminating the need to separate core loss from rotational losses during motor testing. The procedure corresponds to the T-branch presented in the equivalent circuit with only the magnetising reactance X_m . No-load reactance is then as follows.[5]

$$X_{NL} = X_1 + X_m \quad (8)$$

Where no-load reactance is as follows [5].

$$X_{NL} = \frac{Q_{NL}}{3I_1^2} \quad (9)$$

Given that the three-phase apparent power is $S_{NL} = 3V_1I_1$, the no-load reactive power can be determined as follows [5].

$$Q_{NL} = \sqrt{S_{NL}^2 - P_{NL}^2} \quad (10)$$

2.5 Locked-Rotor Test

Rotor resistance R_2 , stator leakage reactance X_1 and rotor leakage reactance X_2 are obtained with the locked-rotor test. With these and earlier parameters, the impedance of the equivalent circuit Z_{LR} can be calculated.[18] During the locked-rotor test the stator voltage V_1 , the stator current I_1 and the three-phase power P_{LR} are measured [5]. Usually, the test is performed by gradually raising the supply voltage until the value of the rated current is obtained, while the rotor of the motor is locked so that it cannot rotate [18]. The current becomes four to eight times higher than the rated current, and windings will be overheated if the rated three-phase voltage V_1 is applied [5].

When the rotor is locked, the slip s equals to 1 and only a small exciting current flows through the exciting branch, leading to minimal flux and core losses. The rotor is not allowed to rotate, so the mechanical speed is zero, and there are no rotational losses. Thus, at a standstill, the power input P_{LR} is mainly dissipated as copper losses in the stator and rotor windings, while core losses are considered negligible.[3,5] Usually, the test is done at a lower frequency f_{LR} so reactances must be scaled to determine the accurate value at the rated frequency f_n .

Typically $f_{LR} = \frac{1}{4}f_n$. However, for induction motors with a rating of less than 20 kW, the frequency effects are negligible, allowing the locked-rotor test to be performed directly at the rated frequency.[5]

Given that the three-phase apparent power is $S_{LR} = 3V_1I_1$, the locked-rotor reactive power can be determined as follows [5].

$$Q_{LR} = \sqrt{S_{LR}^2 - P_{LR}^2} \quad (11)$$

Locked rotor reactance X_{LR} which is corrected for the rated and the resistance R_{LR} can be determined as follows [5].

$$X_{LR} = \frac{f_n Q_{LR}}{f_{LR} 3I_1^2} \quad (12)$$

$$R_{LR} = \frac{P_{LR}}{3I_1^2} \quad (13)$$

As $X_m \gg R_2$ the rotor resistance R_2 and reactance X_2 can be determined as follows [5].

$$R_2 = (R_{LR} - R_1) \left(\frac{X_2 + X_m}{X_m} \right)^2 \quad (14)$$

$$X_2 = (X_{LR} - X_1) \left(\frac{X_m}{X_1 + X_m - X_{LR}} \right) \quad (15)$$

With slip $s=1$ and reactances at rated frequency, the impedance of the equivalent circuit Z_{LR} can be determined as follows [5].

$$Z_{LR} = (R_1 + jX_1 + R_2 + jX_2) \parallel X_m \quad (16)$$

At this stage, only the overall leakage reactance X_{LR} is determined [5]. The calculations begin by assuming a correlation between X_1 and X_2 . When design specifics are available, the computed ratio X_1/X_2 should be used. If not, then Table 1 is used [19].

Table 1. Correlation between stator and rotor leakage reactances [19].

Motor type	X1 / X2
Wound rotor	1.00
Class A	1.00
Class B	0.67
Class C	0.43
Class D	1.00

2.6 Load Test

Three-phase induction motor efficiency is obtained with a load test. The motor is loaded with different loads. With each load, the input power P_{in} , torque T and the actual speed of the rotor N are measured. After measurements, it's possible to draw an efficiency curve and determine

the maximum efficiency. Mechanical output power P_{out} and efficiency η can be then determined as follows.[14,20]

$$P_{out} = \frac{2\pi}{60} NT \quad (17)$$

$$\eta = \frac{P_{out}}{P_{in}} \cdot 100\% \quad (18)$$

2.7 Thévenin's theorem

Thévenin's theorem states that with a voltage source and a resistor in series, any linear active network can always be replaced. The voltage source's electromotive force EMF is equal to the open-circuit voltage of the active two-terminal network, while its equivalent internal resistance is the equivalent resistance when all independent power supplies in the network are replaced by their ideal conditions. This means the ideal current source is regarded as an open circuit, and the ideal voltage source as a short circuit.[21]

To simplify the equivalent circuit of an induction motor, Thévenin's theorem can be used. The formulas based on Thévenin's theorem can be used to help determine the motor's parameters. The voltage V_{th} and impedance Z_{th} resultants can be determined as follows.[5]

$$V_{th} = V_1 \frac{X_m}{\sqrt{R_1^2 + (X_1 + X_m)^2}} \quad (19)$$

$$Z_{th} = R_{th} + jX_{th} = \frac{jX_m(R_1 + jX_1)}{R_1 + j(X_1 + X_m)} \quad (20)$$

The rotor current I_2 amplitude referred to the stator can be determined as follows [5].

$$I_2 = \frac{V_{th}}{\sqrt{\left(R_{th} + \frac{R_2}{s}\right)^2 + (X_{th} + X_2)^2}} \quad (21)$$

The mechanical torque T can be determined as follows [5].

$$T = \frac{3 \frac{R_2}{s} V_{th}^2}{\frac{2\pi}{60} N \left[\left(R_{th} + \frac{R_2}{s}\right)^2 + (X_{th} + X_2)^2 \right]} \quad (22)$$

3 Experimental Setup

3.1 Experimental equipment

The experiments were performed with a semi-automatic electric machines laboratory by De Lorenzo. During experiments, the power supply (DL 10281), loads and rheostats (DL 10283) an electrical measuring unit (DL 10282NF), electromagnetic brake (DL 10300A), mechanical power measurement module (DL 10055NF), load cell (DL 2006D) and the modular system (DL 10280) were used. The equipment used and the modular system parts are presented in Figure 4. De Lorenzo's measurement software was used to collect the data on a computer.

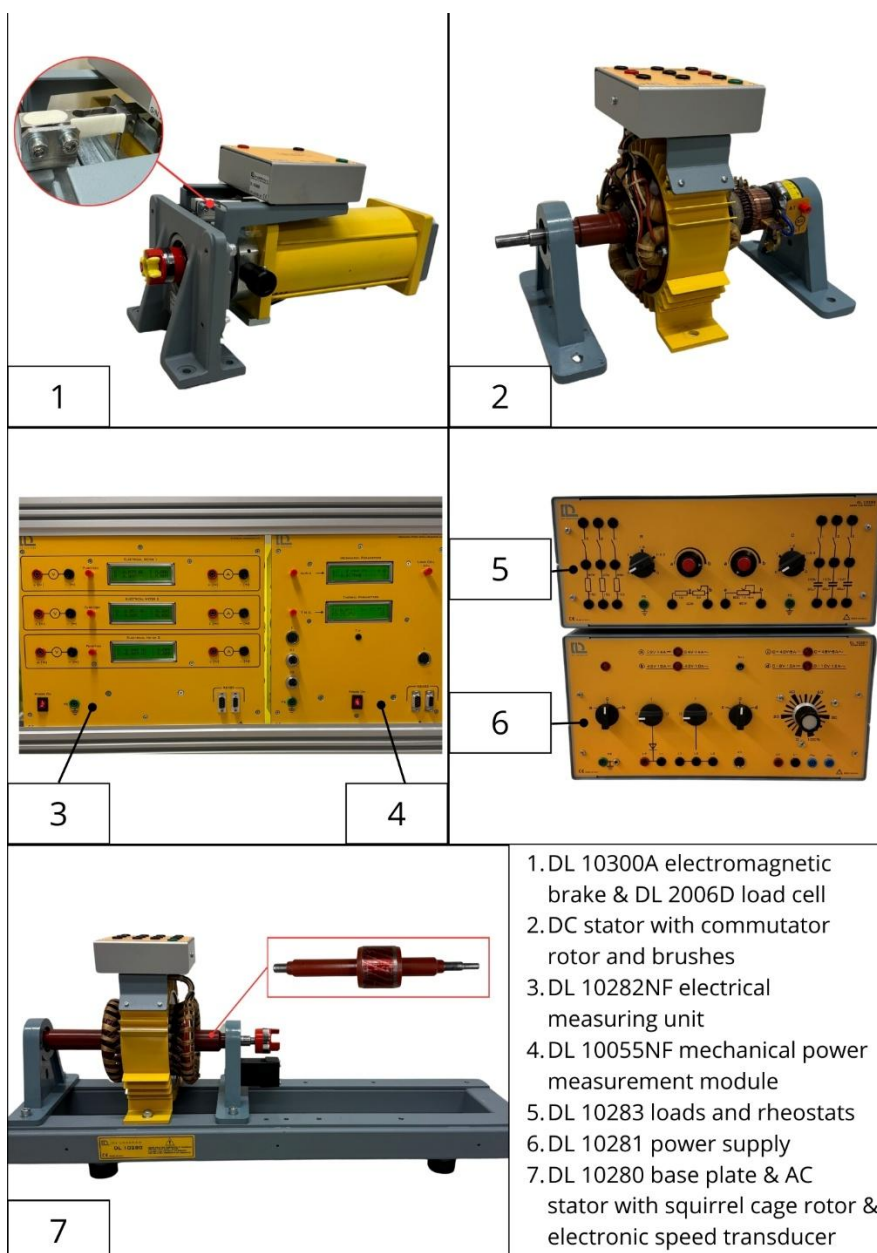


Figure 4. The laboratory equipment used in the experiments.

3.2 Procedure

3.2.1 Test procedure

The tests are based on the principles presented in the literature review (see Chapter 2). Current, voltage and electrical power were measured with an electrical measuring unit. Torque, rotor speed and mechanical power were measured with a mechanical measuring unit. For rotational speed, an electronic speed transducer was also needed. A power supply was used to supply three-phase power to the AC motor's stator and DC power to the DC motor's stator, electromagnetic brake, and AC motor's stator during the direct current resistance test. De Lorenzo's measurement software was used to collect the data from the load and direct current resistance tests. The rest of the results were collected straight from the displays of the measuring units and tabbed into Excel.

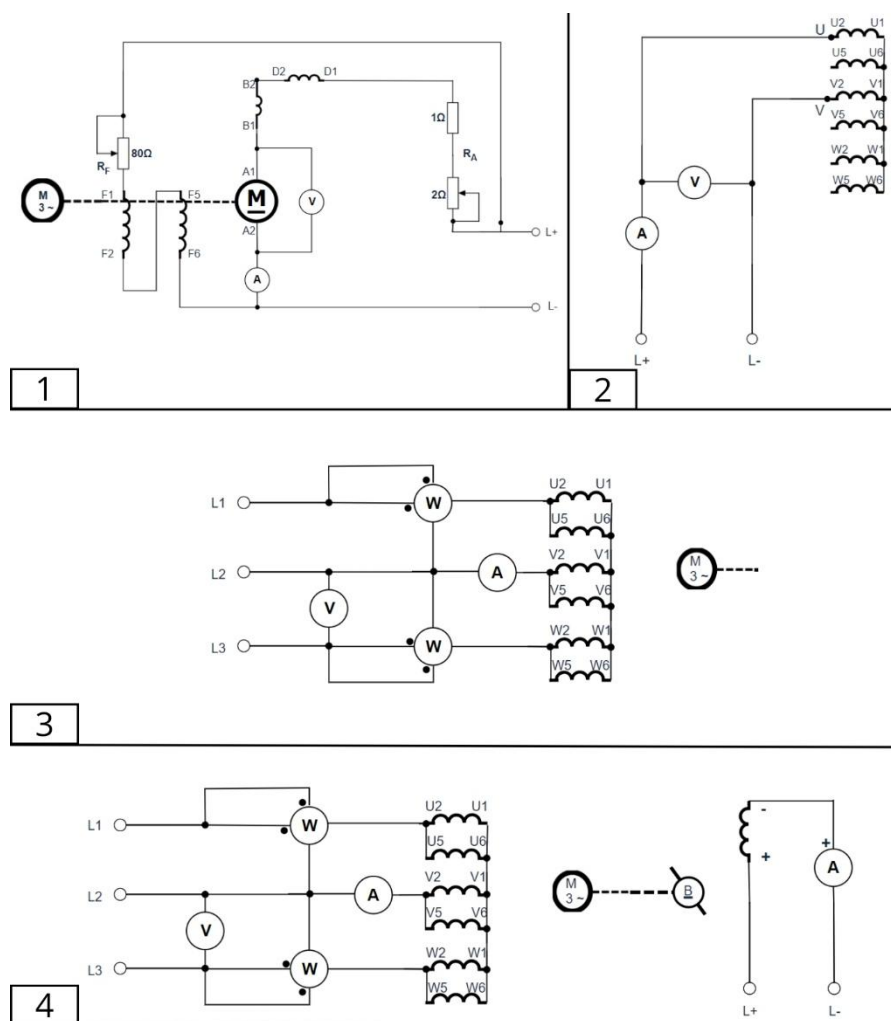
The stator winding is connected to a two-pole double star during the tests. In the direct current resistance test, the resistance of all three terminal sets (U-V, V-W and W-U) was measured, and an average of those three results was used. Rotational losses were measured with a DC motor. A load and rheostat module was used to control the DC motor's rotational speed. The principle for this style to measure rotational losses is presented in Chapter 2.4. De Lorenzo's motor was small enough, so a locked rotor test was possible to perform with rated voltage and frequency. In the load test, the electromagnetic brake was used to add more load to the motor, and torque was measured using a load cell. The electrical diagrams of all tests are presented in Figure 5.

3.2.2 Modelling

The Simcenter SPEED by Siemens were used to model the De Lorenzos' laboratory AC motor. The stator and rotor were measured with a calliper, and all the measurements were input into Simcenter SPEED. Also, multiple other parameters were input into SPEED, including, for example, line voltage, actual rotor speed, synchronous speed, number of poles, number of stator and rotor slots, and winding connection. All the parameters SPEED needs for modelling are not appropriate to list here. After the modelling, SPEED gives the design sheet and multiple plots, which can be used for motor analysis. The relevant parts of the design sheet for this thesis, including equivalent circuit parameters and performance, are presented in Appendix 1.

3.2.3 Results analysis

The MATLAB program was coded to analyse the motor. In coding the MATLAB program, the equations presented in Chapter 2 were used to enable the program to calculate the desired parameters with measured values. During these tests, the ratio between rotor and stator leakage reactance was 1.00. To plot the graphs based on the measured values, Thévenin's theorem was used, excluding the efficiency graph. For comparison between experimental and modelling results, the data from the modelling was exported from Simcenter SPEED to MATLAB, and the graphs were combined. The MATLAB code is in its entirety in Appendix 2.



1. Electrical diagram for the DC motor connection in the rotational loss test
2. Electrical diagram for the direct current resistance test, with stator terminals U-V connected
3. Electrical diagram for the locked rotor test and the no-load test
4. Electrical diagram for the load test

Figure 5. Electrical diagrams of the experiments.

4 Results

The test's measured values are in Tables 2, 3, 4, 5 and 6. Simcenter SPEED results have also been added to Tables 3, 4, and 5. In Table 7, the calculated parameter values and modelled parameter values are listed. Figures 6 and 7 show plots based on the measured and modelled values.

Table 2: Direct current resistance test results.

Measurement number	Measured variable	Stator terminals U-V	Stator terminals V-W	Stator terminals W-U
1	Voltage (V)	0.547	0.561	0.566
1	Current (A)	0.988	1.002	1.008
2	Voltage (V)	1.123	1.078	1.080
2	Current (A)	2.023	1.949	1.931
3	Voltage (V)	1.591	1.609	1.636
3	Current (A)	2.900	2.917	2.930
	Resistance average (Ω)	0.552	0.554	0.559

Table 3: No-load test results.

	Line voltage (V)	Current (A)	Power (W)	Speed (rpm)
Meter 1	28.87	2.867	56.48	
Meter 2	28.76	2.823	-18.54	
Average/total	28.82	2.85	37.94	
Mechanical measuring unit				2982
Simcenter SPEED	28.82	2.18	39.85	2982

Table 4: Rotational losses

	Power without AC motor (W)	Power with AC motor (W)	Rotational losses (W)
DC motor	28.87	45.60	16.73
Simcenter SPEED			16.73

Table 5: Locked-rotor test results.

	Line voltage (V)	Current (A)	Power (W)
Meter 1	25.83	20.44	508.3
Meter 2	25.77	20.43	169.5
Average/total	25.8	20.44	677.8
Simcenter SPEED	25.8	22.09	845.74

Table 6: Load test results.

Speed (rpm)	Power input (W)	Torque (Nm)	Current (A)	Power output (W)	Efficiency (%)
2982	36.220	0.029	2.845	9.054	24.997
2970	60.525	0.097	2.958	30.163	49.836
2946	92.471	0.201	3.244	61.998	67.046
2916	126.897	0.292	3.693	89.149	70.253
2880	164.771	0.388	4.278	116.996	71.005
2868	183.918	0.441	4.621	132.423	72.001
2850	202.096	0.482	4.950	143.826	71.167
2814	243.263	0.578	5.722	170.294	70.004
2760	290.775	0.684	6.797	197.657	67.976
2718	331.122	0.782	7.783	222.537	67.207

Table 7: Obtained values.

	Experimental results	Simcenter SPEED results
$X_1 (\Omega)$	0.25	0.2035
$X_2 (\Omega)$	0.25	0.2365
$X_m (\Omega)$	5.38	7.3420
$R_1 (\Omega)$	0.28	0.3749
$R_2 (\Omega)$	0.29	0.1682
$P_{rot} (W)$	16.73	16.73
$R_c (\Omega)$	52.93	100.4269
$Z (\Omega)$	$0.54009 + 0.48232j$	$0.53269 + 0.42446j$

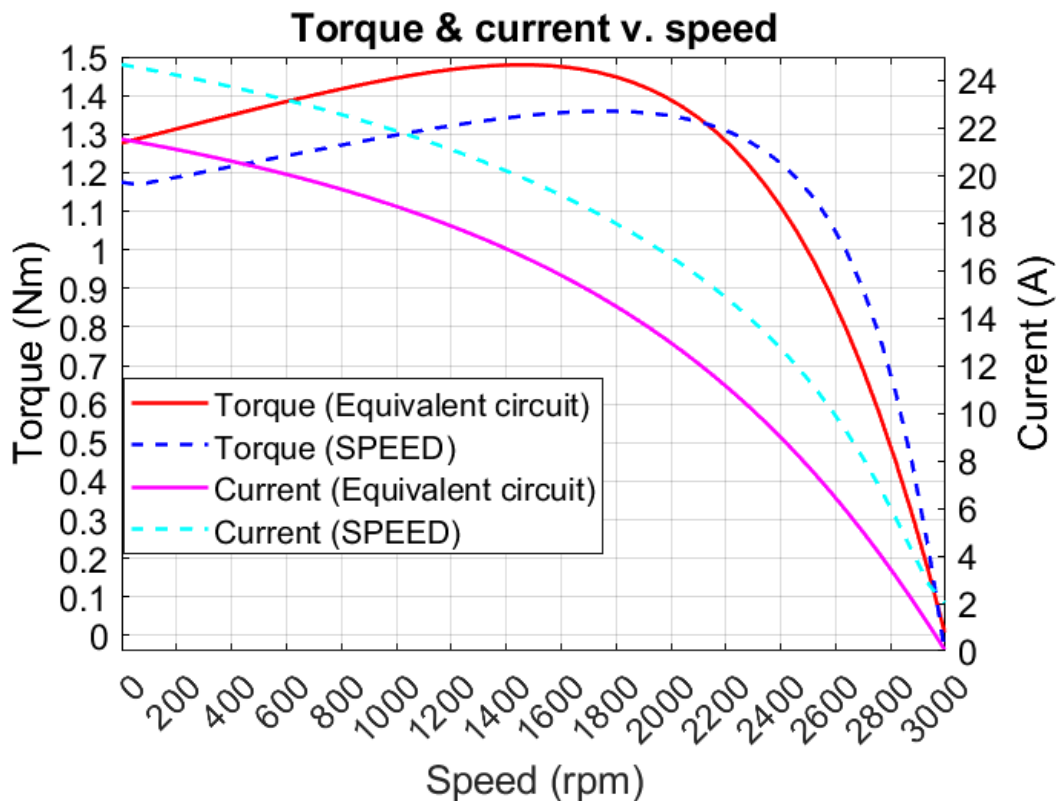


Figure 6. Plot comparing the equivalent circuit to SPEED.

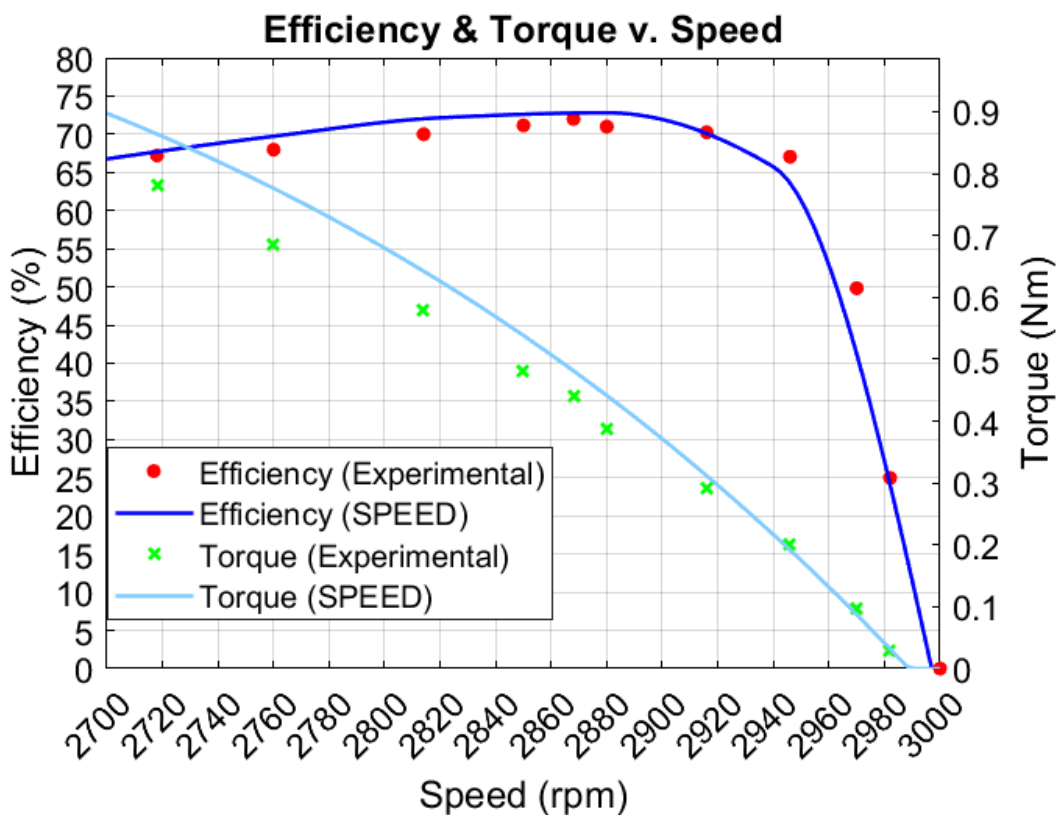


Figure 7. Plot comparing load test experimental results to SPEED.

5 Discussion

As we can see, some differences exist between the experimental parameter values and the modelled parameter values. There is about 0.13 ohms difference between the rotor resistance values and 0.09 ohms difference between the stator resistance values. Differences in leakage reactances are 0.2-0.5 ohms, with a magnetising reactance difference is about 2 ohms.

Rotational losses are the same because this is a parameter that is input into SPEED. The difference between core loss resistances is significant, almost 50 ohms. With impedance, the real part (resistance) difference is about 0.01 ohms and the imaginary part (reactance) difference is about 0.06 ohms.

Because there are some differences in parameters, there are also some differences in plots. In the current v. speed plot, the modelled value at 0 rpm is about two amps higher. The modelled value always remains higher, but the difference decreases as the rotor speed approaches 3000 rpm. The experimental value in the torque v. speed plot is higher at the beginning than the modelled value. Also, the experimental curve reaches the highest torque value at 300-400 rpm earlier than the modelled curve. After curves crossing around 2100 rpm, the modelled values remain slightly higher than the experimental values. In the efficiency v. speed plot, the curves are almost identical.

Many factors can explain differences in parameter values and plot lines. The experimental tests that are conducted work better with larger machines. The test laboratory machine is tiny, compared to industrial-scale induction machines. Also, the calibration level of the test equipment can cause some uncertainties in the measured results. The way the desired parameters are calculated varies between modelling and experimental results calculation. Simcenter SPEED use more advanced ways to calculate parameters, and the method expressed in Chapter 2 is more approximate. Modelling with Simcenter SPEED requires multiple accurate parameters to be input into the software. Even small differences in those parameters can cause differences between experimental and modelled values.

6 Conclusion

In this thesis, we focused on a three-phase induction motor with a squirrel cage rotor. The motor model parameters were determined experimentally and by modelling. The MATLAB program was coded to analyse experimental results and combine plots. The possible factors for uncertainties between modelled and experimentally calculated values were determined. This thesis combines theoretical modelling with practical work. It's shown that commercial motor design software is also an effective tool for educational purposes and for analysing the teaching laboratories.

For future work, the analysis could be extended to different motor types, such as an induction motor with a wound rotor. Also, various operating conditions or environments could be the subject of closer examination. Minimising the uncertainties in experimental work and modelling might also be a good subject to focus on more.

In conclusion, the three-phase induction motor can be modelled experimentally and with modelling software. And with the same motor, it's possible to get almost the same parameters both ways. As mentioned earlier, the result might be closer with larger motors, but even with the small machine, it's possible to get reliable results.

7 References

- [1] Ma W, Bai L. Overview of Three-Phase Asynchronous Motors. *Energy-Saving Principles and Technologies for Induction Motors*, John Wiley & Sons; 2018, p. 11–55.
- [2] Anthony Z, Nazir R, Hamid MI. A Review of Strategies for Improving 3-Phase Induction Motor Performance. *Andalasian International Journal of Applied Science, Engineering and Technology* 2024;4:01–12. <https://doi.org/10.25077/aijaset.v4i1.112>.
- [3] Sengamalai U, Anbazhagan G, Thamizh Thentral TM, Vishnuram P, Khurshaid T, Kamel S. Three Phase Induction Motor Drive: A Systematic Review on Dynamic Modeling, Parameter Estimation, and Control Schemes. *Energies* 2022;15:8260. <https://doi.org/10.3390/en15218260>.
- [4] Iqbal A, Moinoddin S, Reddy BP. Three-Phase Induction Machine. *Electrical Machine Fundamentals with Numerical Simulation Using MATLAB / SIMULINK*, Newark, UNITED KINGDOM: John Wiley & Sons, Incorporated; 2021, p. 401–89.
- [5] Figueiredo EF. Rotating Electrical Machines. In: Papailiou KO, editor. *Springer Handbook of Power Systems*, Singapore: Springer Singapore; 2021, p. 367–441. https://doi.org/10.1007/978-981-32-9938-2_6.
- [6] Sivaraman P, Sharmeela C, Nayagi AT, Mahendran R. 4. AC Machines. *Basic Electrical and Instrumentation Engineering*, John Wiley & Sons; 2021, p. 185–238.
- [7] Deng X, Mecrow B. Electrical machines for an integrated drive. *Integrated Motor Drives*, Institution of Engineering and Technology (The IET); 2022, p. 17–55.
- [8] Patrick DR, Fardo SW, Richardson RE, Chandra V (Vigs). Hysteresis Loss. *DC/AC Electrical Fundamentals*, River Publishers; 2022, p. 418–20.
- [9] Li S, Zhu N, Wei B, Fu Y. On-Line Parameter Identification of a Squirrel Cage Induction Motor. *J Phys: Conf Ser* 2019;1302:022054. <https://doi.org/10.1088/1742-6596/1302/2/022054>.
- [10] WEF. Three-phase alternating current motors. *Wastewater Treatment Fundamentals II - Solids Handling and Support Systems*, Water Environment Federation (WEF); 2021, p. 349–50.
- [11] Aishwarya M, Brisilla RM. Design of Energy-Efficient Induction motor using ANSYS software. *Results in Engineering* 2022;16:100616. <https://doi.org/10.1016/j.rineng.2022.100616>.

- [12] Anthony Z, Bandri S, Erhaneli E, Warmi Y, Zulkarnaini Z, Rachman AYD. A winding design for improving 3-phase induction motor performance. *International Journal of Electrical and Computer Engineering (IJECE)* 2024;14:2413–21. <https://doi.org/10.11591/ijece.v14i3.pp2413-2421>.
- [13] Rauf SB. *Electric Motors and Generator. Electrical Engineering for Non-Electrical Engineers (3rd Edition)*, River Publishers; 2021, p. 209–34.
- [14] Niazi MA, Hayat Q, Khan B, Afaq M. Speed Control of Three Phase Induction Motor using Variable Frequency Derive Control System. *IJCET* 2021;10:5–10. <https://doi.org/10.14741/ijcet/v.10.1.2>.
- [15] Tleis N. *Modelling of rotating ac synchronous and induction machines. Power Systems Modelling and Fault Analysis - Theory and Practice (2nd Edition)*, Elsevier; 2019, p. 371–468.
- [16] Dianov A, Anuchin A. Offline Measurement of Stator Resistance and Inverter Voltage Drop Using Least Squares. *IEEE Access* 2023;11:17053–65. <https://doi.org/10.1109/ACCESS.2023.3245663>.
- [17] Morfin OA, Castaneda CE, Ruiz-Cruz R, Valenzuela FA, Murillo MA, Quezada AE, et al. The Squirrel-Cage Induction Motor Model and Its Parameter Identification Via Steady and Dynamic Tests. *Electr Power Compon Syst* 2018;46:302–15. <https://doi.org/10.1080/15325008.2018.1445140>.
- [18] Makinde KA, Bakare MS, Akinloye BO, Amole AO, Adewuyi OB, Zubair UO, et al. Simulation based testing and performance investigation of induction motor drives using matlab simulink. *SN Appl Sci* 2023;5:73. <https://doi.org/10.1007/s42452-023-05296-w>.
- [19] *IEEE Standard Test Procedure for Polyphase Induction Motors and Generators* 2018. <https://doi.org/10.1109/IEEESTD.2018.8291810>.
- [20] Kosky P, Balmer R, Keat W, Wise G. *Design Step 4: Detailed Design. Exploring Engineering - An Introduction to Engineering and Design (5th Edition)*. 5th ed., Elsevier; 2021, p. 541–56.
- [21] Fan Y, Hu Y, Li J. Thevenin Theorem and Norton's Theorem. *2022 IEEE 2nd International Conference on Electronic Technology, Communication and Information (ICETCI)*, 2022, p. 142–4. <https://doi.org/10.1109/ICETCI55101.2022.9832065>.

Appendices

Appendix 1. Simcenter SPEED design sheets

```

5 Equivalent circuit parameters : -----
R1          0.3749 ohm   X1          0.2035 ohm   Xlunsat     0.2035 ohm
R2          0.1682 ohm   X2          0.2365 ohm   X2unsat     0.2365 ohm
Rc         100.4269 ohm  Xm0         9.5462 ohm   Xm          7.3420 ohm
Rbar        0.0523 ohm   REndRing    0.1159 ohm   Erb         0.0000 V
R_rotor     9.4051E-05 ohm X_rotor     1.3224E-04 ohm XErb        1.0000
EQcct       SPEED      RCLoc       GapFlux
DeepBar     Classical   K_r         1.0000       K_x         1.0000
EndLeak     CGV        XKr_DB      1.0000       XKx_DB      1.0000
CoilFill    1.0000     kEndCoil    1.0000       kEndCoil    1.0000
XXlend      1.0000     XX2end      1.0000       XX2end      1.0000
DiffLeak    CGV        DiffSat     false        Alzz        Normal
LkSat       None       kXL1        1.0000       kXL2        1.0000
kzz         1.0000     kX1slot     1.0000       kX2slot     1.0000
Xkzz        1.0000     XkX1slot    1.0000       XkX2slot    1.0000
XXm         1.0000     XXL1        1.0000       XXL2        1.0000
XXlend      1.0000     XX2end      1.0000

Unsaturated reactance components..
X1slot      0.0480 ohm   Xlend       0.0743 ohm   Xldiff      0.0812 ohm
X1belt      0.0273 ohm   X1zz        0.0539 ohm   X1skew      0.0000 ohm
X2slot      0.0476 ohm   X2end       0.0000 ohm   X2diff      0.1890 ohm
X2belt      0.0273 ohm   X2zz        0.0539 ohm   X2skew      0.0000 ohm

L-circuit parameters..
alpha_TL    1.0322          uX1oX2      1.0000       X1oX2       0.8603
XL_L        0.4620 ohm  Rc_L        107.0016 ohm
R2_L        0.1792 ohm  Xm_L        7.5785 ohm

6 Performance : -----
OpMode      Motoring
Vt          28.8200 V   rpm         2982.0000 rpm   Slip         0.0060 p.u.
Pshaft     10.2089 W   PElec       39.8466 W   Tshaft      0.0327 Nm
PshaftHP   0.0137 h.p.   P.F.        0.3777     Effcy       25.6204 %
WTotals    29.6442 W   Eff_X_PF    9.6757 %

Currents..
Iph1       2.1137 A rms  IL1         2.1137 A rms  I2           0.5689 A rms
Imc        2.1785 A rms  IMag        2.1727 A rms  Ic           0.1587 A rms

Equivalent circuit voltages..
E1         15.9520 V   VR1         0.7925 V   VX1          0.4301 V
ER2        15.8557 V   VR2         0.0957 V   VX2          0.1346 V

Losses and related parameters..
WCuS       5.0253 W   WCuR        0.1634 W   WIron        7.6015 W
SLLCalc    ANSIC50     WSLl        0.1240 W
Wwf        16.7300 W   W_brg       0.0000 W
Jrms       1.2205 A/mm^2
JBar1      0.1412 A/mm^2  J_ER        0.3143 A/mm^2  JRotor       0.2037 A/mm^2

Other performance parameters..
PGap       27.2262 W   EMTorque    0.0867 Nm

Test data..
V_Test     240.0000 V   I_Test      0.0000 A rms  P_Test       0.0000 W
f_Test     50.0000 Hz   s_Test      0.0000 p.u.
T1_Test    20.0000 °C   T2_Test     20.0000 °C

```

Figure 8. Equivalent circuit and performance parts from the design sheet.

Appendix 2. The MATLAB code

```

clc;
clear;
params = struct();
% Parameters measured in the tests
fprintf('Enter the parameters obtained from the no-load test \n');
params.V1 = input('V1 (V/phase): ');
params.I1 = input('I1 (A): ');
params.P1 = input('P1 (W): ');
params.N_synchronous = input('N_synchronous (rpm): ');
fprintf('Enter the parameters obtained from the locked-rotor test \n');
params.V2 = input('V2 (V/phase): ');
params.I2 = input('I2 (A): ');
params.P2 = input('P2 (W): ');
params.correlation = input('Enter correlation X1/X2: ');
fprintf('Enter the parameters obtained from the direct current resistance test \n');
params.R_av = input('R_av ( $\Omega$ ): ');
winding_sd = input('Is the stator star- or delta-connected? (enter "star" or "delta": ', 's');
if strcmpi(winding_sd, 'star')
    params.winding = 0.5;
elseif strcmpi(winding_sd, 'delta')
    params.winding = 1.5;
else
    error('Invalid input! Please enter "star" or "delta"');
end
fprintf('Enter the rotational losses \n');
params.P_rot = input('P_rot (W): ');
continueLoop = true;
while continueLoop
    % No-load and locked-rotor reactances and reactive powers
    Q_lr = sqrt((3*params.V2*params.I2)^2 - params.P2^2);
    Q_nl = sqrt((3*params.V1*params.I1)^2 - params.P1^2);
    X_lr = Q_lr / (3*params.I2^2);
    X_nl = Q_nl / (3*params.I1^2);
    % Rotor reactance
    syms X2;
    eq = X2 == (X_lr - (params.correlation * X2)) * ((X_nl - (params.correlation * X2)) / ((params.correlation * X2) + (X_nl - (params.correlation * X2)) - X_lr));
    sol = solve(eq, X2);
    sol1 = simplify(sol(1));
    sol2 = simplify(sol(2));
    numeric_sol1 = double(sol1);
    numeric_sol2 = double(sol2);
    if numeric_sol1 < numeric_sol2
        X2_correct = sol1;
    end
end

```

```

else
    X2_correct = sol2;
end
% Stator reactance and magnetizing reactance
X1 = params.correlation * X2_correct;
X_m = X_n1 - X1;
% Resistance calculations
R_lr = (params.P2) / (3 * params.I2^2);
R1 = params.winding * params.R_av;
R2 = (R_lr - R1) * ((X2_correct + X_m) / (X_m))^2;
% Impedance calculation
s = 1;
term1 = R1 * ( (R2 / s)^2 + (X2_correct + X_m)^2 );
term2 = (R2 * X_m^2) / s;
term3 = X_m * ((R2 / s)^2 + X2_correct^2 + X2_correct * X_m);
term4 = X1 * ((R2 / s)^2 + (X2_correct + X_m)^2);
numerator_real = term1 + term2;
numerator_imag = term3 + term4;
denominator = (R2 / s)^2 + (X2_correct + X_m)^2;
Z = (numerator_real + 1i * numerator_imag) / denominator;
% Core loss and core loss resistance
P_core = params.P1 - (3*params.I1^2*R1) - params.P_rot;
R_c = 3 * ((params.V1 - (params.I1 * X1))^2 / P_core);
% Results
fprintf('\nResults:\n');
fprintf('-----\n');
fprintf('X1 (Stator leakage reactance): %.2f Ω\n', double(X1));
fprintf('X2 (Rotor leakage reactance): %.2f Ω\n', double(X2_correct));
fprintf('X_m (Magnetizing reactance): %.2f Ω\n', double(X_m));
fprintf('R1 (Stator resistance): %.2f Ω\n', R1);
fprintf('R2 (Rotor resistance): %.2f Ω\n', R2);
fprintf('P_rot (Rotational losses): %.2f W\n', params.P_rot);
fprintf('R_c (Core loss resistance): %.2f Ω\n', R_c);
fprintf('Z (Impedance): %.5f + %.5fj Ω\n', real(Z), imag(Z));
% Torque, current-speed plots
w_synchronous = (params.N_synchronous * 2 * pi) / 60;
V_th = params.V1 * (X_m / sqrt(R1^2 + (X1 + X_m)^2));
Z_th = ((1i*X_m) * (R1 + 1i*X1)) / (R1 + 1i*(X1 + X_m));
R_th = real(Z_th);
X_th = imag(Z_th);
s = (0:1:50) / 50;
s(1) = 0.001;
N = (1-s) * params.N_synchronous;
for i = 1:51
    T(i) = (3 * V_th^2 * R2 / s(i)) / (w_synchronous * ((R_th + R2/s(i))^2 + (X_th + X2_correct)^2)); %Torque
    I2(i) = V_th / sqrt((R_th + R2 / s(i))^2 + (X_th + X2_correct)^2); %Stator
current
end

```

```

%Plots with simcenter speed
data = readmatrix('TSCHARS.txt');
D = data(:,4);
D2 = data(:,2);
figure;
plot(D, D2, 'b', 'LineWidth', 1.5);
xlabel('Speed (rpm)');
ylabel('Torque (Nm)');
title('Torque v. speed','FontWeight','bold');
grid on;
hold on;
plot(N, T, 'r', 'LineWidth', 1.5);
xticks(0:200:3000);
yticks(0:0.1:1.5);
legend('SPEED','Equivalent circuit','Location','Best');
hold off;
data = readmatrix('TSCHARS.txt');
D3 = data(:,4);
D4 = data(:,6);
figure;
plot(D3, D4, 'c', 'LineWidth', 1.5);
xlabel('Speed (rpm)');
ylabel('Current (A)');
title('Current v. speed','FontWeight','bold');
grid on;
hold on;
plot(N, I2, 'm', 'LineWidth', 1.5);
xticks(0:150:3000);
yticks(0:2:25);
legend('SPEED','Equivalent circuit','Location','Best');
hold off;
figure;
yyaxis left
plot(N, T, 'LineWidth', 1.5, 'Color', 'r');
hold on;
plot(D, D2, 'b', 'LineWidth', 1.5);
ylabel('Torque (Nm)')
ax = gca;
ax.YColor = 'k';
yticks(0:0.1:1.5)
yyaxis right
plot(N, I2, 'LineWidth', 1.5, 'Color', 'm');
hold on;
plot(D3, D4, 'c', 'LineWidth', 1.5);
ylabel('Current (A)')
ax.YColor = 'k';
yticks(0:2:25)
hold off;
xlabel('Speed (rpm)');

```

```

title('Torque & current v. speed', 'Fontweight', 'Bold');
xticks(0:200:3000)
grid on;
legend('Torque (Equivalent circuit)', 'Torque (SPEED)', 'Current (Equivalent
circuit)', 'Current (SPEED)', 'Location', 'Best');
%Efficiency plot with simcenter speed
data = readmatrix('TSCHARS.txt');
min_value = 2700;
max_value = 3000;
efficiency = [0, 24.977, 49.836, 67.046, 70.253, 71.005, 72.001, 71.167, 70.004,
67.976, 67.207];
rpm = [3000, 2982, 2970, 2946, 2916, 2880, 2868, 2850, 2814, 2760, 2718];
filtered_data = data(data(:,4) >= min_value & data(:,4) <= max_value, :);
rpm_interp = linspace(2700, max(rpm), 100);
efficiency_interp = interp1(rpm, efficiency, rpm_interp, 'pchip', 'extrap');
filtered_rpm = filtered_data(:,4);
filtered_efficiency = filtered_data(:,7);
filtered_efficiency_interp = interp1(filtered_rpm, filtered_efficiency, rpm_interp,
'pchip', 'extrap');
efficiency_interp(efficiency_interp < 0) = 0;
filtered_efficiency_interp(filtered_efficiency_interp < 0) = 0;
figure;
plot(rpm_interp, efficiency_interp, 'r', 'LineWidth', 1.5);
hold on;
plot(rpm_interp, filtered_efficiency_interp, 'b', 'LineWidth', 1.5);
xlabel('Speed (rpm)');
ylabel('Efficiency (%)');
title('Efficiency v. Speed');
grid on;
legend('Equivalent circuit', 'SPEED');
xticks(2700:20:3000);
yticks(0:5:80);
hold off;
% Value chancing
answer = input('\nDo you want to modify any values? (yes/no): ', 's');
if strcmpi(answer, 'yes')
    fields = fieldnames(params);
    fprintf('\nSelect a value to modify:\n');
    for i = 1:length(fields)
        fprintf('%d: %s = %.4f\n', i, fields{i}, params.(fields{i}));
    end
    idx = input('Enter the number of the value to modify: ');
    if idx >= 1 && idx <= length(fields)
        fieldname = fields{idx};
        % Special handling for winding changes
        if strcmp(fieldname, 'winding')
            while true
                winding_sd = input('Is the stator connected in "star" or
"delta"? ', 's');

```

```
        if strcmpi(winding_sd, 'star')
            params.winding = 0.5;
            break;
        elseif strcmpi(winding_sd, 'delta')
            params.winding = 1.5;
            break;
        else
            disp('Invalid input! Please enter "star" or "delta".');
        end
    end
else
    newValue = input(['Enter new value for ', fieldname, ': '], 's');
    numericValue = str2double(newValue);
    if isnan(numericValue)
        disp('Invalid number!');
    else
        params.(fieldname) = numericValue;
    end
end
else
    disp('Invalid selection.');
```

```
end
else
    continueLoop = false
```